To be presented at the SEM Annual Conference & Exposition on Experimental and Applied Mechanics, Hyatt Regency Albuquerque, Albuquerque, New Mexico USA, June 1 - 4, 2009, Paper No. 413.

Fluid-structure interaction in liquid-filled composite tubes under impulsive loading

Kazuaki Inaba, Assistant Professor, Tokyo Institute of Technology
2-12-1 Ookayama, Meguro-ku, Tokyo, 152-8550, JAPAN
E-mail: inaba@mech.titech.ac.jp

Joseph E. Shepherd, Professor, California Institute of Technology
1200 E California Blvd, Pasadena, CA 91125, USA
E-mail: joseph.e.shepherd@caltech.edu

ABSTRACT

We are carrying out experiments in our laboratory on fluid-structure interaction generated by impulsive impact on water-filled composite tubes. This is an extension of our previous work on water-filled steel and aluminum tubes. In the present study we have examined the effect of winding angle and fiber lay-up patterns on the wave propagation process. We have tested carbon-fiber reinforced plastic tubes with 45° and 60° winding angles, and glass reinforced plastic with a 50° winding angle, all of 40 mm diameter and between 1.6-1.7 mm wall thicknesses. A 50 mm diameter steel impactor is accelerated to 5 m/s and strikes a polycarbonate buffer within the tube located at the top of the water surface. Strain gages measure hoop and axial strains every 100 mm. We observe primary and precursor waves qualitatively similar to our previous work with metal tubes and the water hammer theory of Skalak. For the same pressure amplitude, the hoop strains are larger in composite tubes than in metal tubes. The relationships between axial and hoop strains are significantly different in the composite tubes than metal tubes due to the anisotropy of the composite material stiffness. The ratio between hoop and axial strain peaks is close to -1 with 45° tubes, the magnitude of axial strains become larger than that of the hoop strains for the 60° tubes. Precursor waves in the 60° tube propagate slower than those for the 45° tube while the primary wave with 60° tube propagates faster than that with the 45° tube. The laminate model of composites and the concept of effective modulus is used to explain these findings.

1 Introduction

The propagation of coupled fluid and solid stress waves in liquid-filled tubes is directly relevant to the common industrial problem of water hammer [1] and also serves as a model for the impact of shock waves on marine structures. When a shock in a liquid propagates perpendicular to submerged structure, flexural waves are generated in the structure. The main wave propagation mode is flexural wave in the structure which can be closely coupled to a pressure wave in the liquid. To investigate this type of coupling, we are using projectile impact and thin-wall water-filled tubes to generate stress waves in the water that excite flexural waves in the tube wall, see Fig. 1.

We have been using this configuration to study [2, 3] elastic and plastic waves in water-filled metal and polymer tubes. The theory of water hammer and our previous studies show that the extent of fluid-solid coupling in this geometry is determined by a nondimensional parameter.

$$\beta = \frac{KD}{Eh} \tag{1}$$

where K is the fluid bulk modulus, E is the solid Young's modulus, D is the tube diameter, and h is the wall thickness. In this case, the coupling is independent of the blast wave characteristics and only depends on the fluid

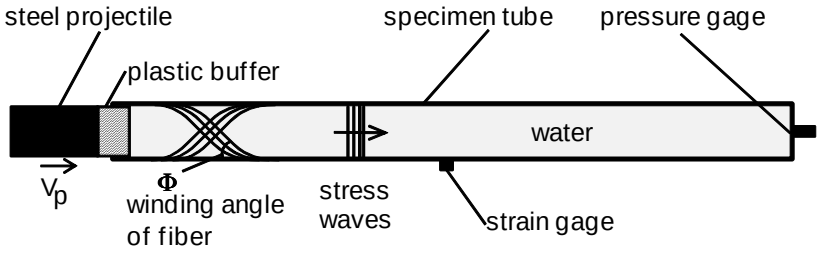

Figure 1: Schematic diagram of axi-symmetric water-in-tube configuration for generation of tube flexural waves coupled with stress waves propagating in the water.

and solid properties and geometry. The Korteweg waves travel at a speed (Lighthill [4])

$$c = \frac{a_f}{\sqrt{1+\beta}} \tag{2}$$

which, depending on the magnitude of β, can be significantly less than the sound speed a_f in the fluid or the bar wave speed $\sqrt{E/\rho_s}$ in the tube. The parameter β is sufficiently large in our experiments that we obtain significant fluid-solid coupling effects. Previous experiments in our laboratory [5] on flexural waves excited by gaseous detonation are superficially similar to the present study but these have all been in the regime of small β.

The current study reports results for elastic wave propagation generated by low-speed impacts. In a companion study [6], we report the results of high-speed impact tests that created damage or complete failure of the composite tubes. The present work extends in a systematic fashion our previous studies [2, 3] in which we used metal tubes or commercial composite tubes which were consisted of an axial fiber core with a woven cloth over-wrap and vinylester resin. In that work, we found [3] that the axial strain is a much smaller fraction (1/10) of the hoop strain than for the aluminum tubes. In the present study, we used filament wound specimen tubes so that a much larger coupling between hoop and axial motion is anticipated and also the fiber and matrix properties were better known than in the previous testing. We have interpreted our results using laminate models composite to predict effective tube modulus (hoop and axial) as a function of the fiber winding angle.

Experimental apparatus and test procedure

Gas gun

As part of our research program on fluid-structure interaction, we designed and built an air cannon (Fig. 2) that is capable of projectile exit velocities more than 200 m/s and a barrel diameter of 50 mm. The air cannon is mounted vertically above a specimen tube filled with water. The 1.5 kg steel projectile is accelerated by a combination of gravity and compressed air using reservoir pressures, up to 16 MPa. In the present phase of our study, we did not use the air reservoir but simply dropped the projectile from the top end of the barrel to obtain an average buffer speed of 5.3 m/s immediately after the impact. This approach results in more reliable low speed impacts since the gland seals between the projectile and tube can be removed, greatly reducing the effects of friction on terminal projectile speed.

The projectile is not completely ejected from the barrel when it impacts a polycarbonate buffer placed on the water surface (see Fig. 2). A gland seal is used to prevent water moving through the clearance space between the buffer and specimen tube. In this fashion, the stress waves due to the impact of the projectile are transmitted directly to the water surface inside the specimen tube. This prevents the projectile from impacting the specimen tube directly and enables us to measure the wave velocities without interference from axial waves created by the projectile impact on the tube itself.

The impact-generated stress waves in the water cause the tube to deform and the resulting coupled fluid-solid motion propagates along the tube and within the water. The deformation of the tube is measured by strain gages oriented in the hoop and axial directions and the pressure in the water is measured by a piezoelectric transducer mounted in an aluminum fitting sealed to the bottom of the tube. The bottom of the tube is fastened to an aluminum bar mounted in a lathe chuck that is placed directly on the floor. A speed of 5.3 m/s is sufficient to obtain peak hoop strains of up to 5 $m$strain (.005) and pressures of 10-15 MPa at the bottom of the tube.

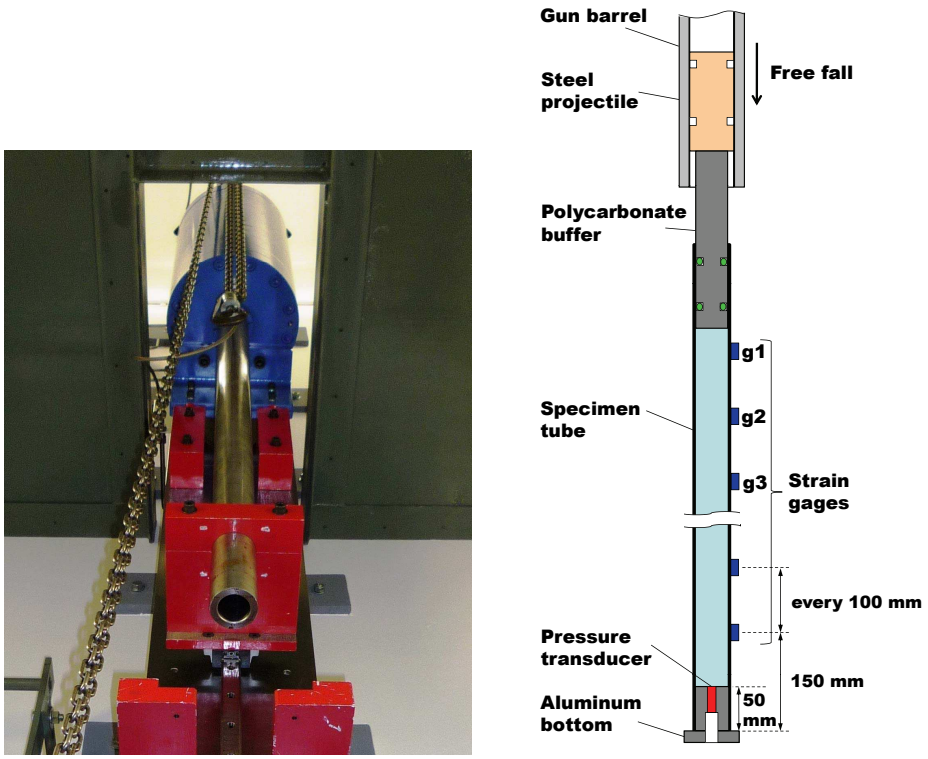

Figure 2: Picture of GALCIT 2-in gas gun mounted vertically in Explosion Dynamics Laboratory and schematic of test specimen tube with projectile, buffer, pressure transducer, and strain gages.

Test conditions and specimens

We examined in our tests two types of specimens constructed either with glass reinforced plastic (GRP) or carbon-fiber reinforced plastic (CRP) construction with three winding angles. Nominal wall-thickness and inner diameter are listed in the Table 1. The length of all specimen tubes is 0.9 m. Shot 066 was carried out using a specimen tube consisting of roll-wrapped CFC sheets. Shots 069, 070, and 106 were carried out with a CFC tube which has a winding angle of 60° and woven pattern I as shown in Fig. 3. All CFC tubes were manufactured by Black Project^{TM} and consisted of carbon fibers (Toho Tenax, HTS 5631-12K) and thermosetting epoxy matrix resin (TCR^{TM} Prepregs, UF3325). Shots 075 and 104, 110 and 108 were conducted with specimens of 45° winding angle and woven patterns I, II, or III. Depending on the pattern, the wall-thickness varies: pattern I, 1.66 mm; pattern II, 1.59 mm, pattern III, 1.74 mm. Finally, Shots 112 and 113 were performed with a glass reinforced plastic tube, winding angle of 50° (Airframe Tubes by Hawk Mountain Enterprises).

Each test specimen is instrumented at 100 mm increments with 12-14 strain gauges for measuring hoop and axial

Table 1: Test Matrix.

Shot	Tube	Winding angle, $\pm\Phi$ [deg]	Wall-thickness [mm]	Inner diameter [mm]
066	CFC#7	45*	1.74	38.3
069,070	CFC#8	60	1.65	38.3
075	CFC#4-1	45	1.66	38.3
104,110	CFC#5-1,2	45	1.59	38.3
106	CFC#9	60	1.65	38.3
108	CFC#6-1	45	1.74	38.3
112,113	GRP#3	50	1.60	38.8

*Roll-wrapped sheet, ply angle

strains. A single piezoelectric pressure transducer recorded the pressure wave reflected from the aluminum plug at the bottom of the specimen. A high-speed video camera (Vision Research Phantom v7.3) is used to observe the buffer motion due to the projectile impact and determine the buffer speeds by postprocessing the images.

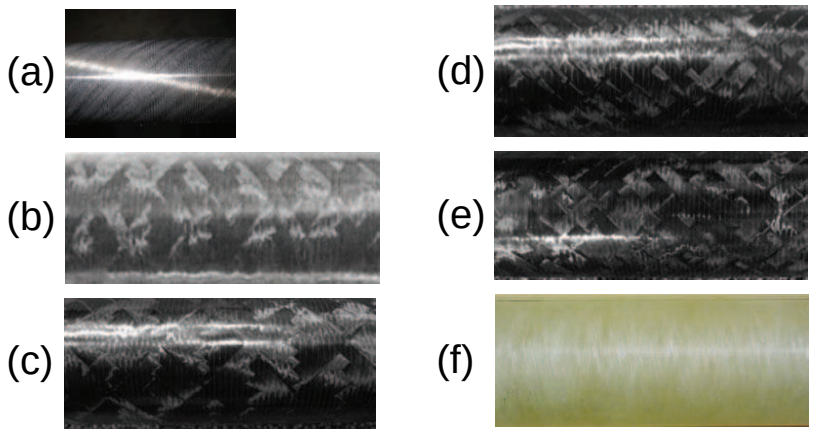

Figure 3: Test specimen tubes (a) CFC#7, roll-wrapped sheet with ply angle of 45°, (b) CFC#8,9, $\Phi = 60°$, pattern I, (c) CFC#4-1, $\Phi = 45°$, pattern I, (d) CFC#5-1,2, $\Phi = 45°$, pattern II (e) CFC#6-1, $\Phi = 45°$, pattern III, (f) GRP#3, $\Phi = 50°$.

2 Results and discussion

Dynamic response of composite tubes

Figure 4 shows hoop and axial (labeled longitudinal in the figures) strain histories measured at locations g1 (bottom trace) to g7 as given in Fig. 2. The top trace in Fig. 4a is the pressure history and since this is obtained in the solid end wall, the pressure values are enhanced over those for the propagating wave due to the effects of reflection at the aluminum-water interface. In Fig. 4, the strain signal baselines are offset proportional to the distance between the gages so that we can also interpret the trajectories of signal features by considering the ordinate as a space location as well as a signal amplitude. The lines labeled 3686 m/s and 675 m/s indicate the leading edge of the precursor wave and the primary (main) stress wave fronts, respectively. The subsequent reflection of the primary waves from the bottom and re-reflection from the buffer can be observed as distinct strain pulses. The averaged peak strains at the primary wave front from all seven 7 hoop and axial gauges in shot 075 are 3.3 $m$strain and -2.7 $m$strain (1 $m$strain $= 10^{-3}$). The values of the peak strains gradually decrease as the wave moves from the impact point toward the bottom. In comparison with the results for metal tubes [2], the hoop strains histories are similar for metal and composite tubes but axial strains are much larger relative to the hoop strains for the composite case. As in the case of water-metal filled tubes, the hoop strains are less oscillatory than observed in the case of gaseous detonation-excited flexural waves [7, 8].

The increased axial strain can be explained by considering how the applied internal pressure load is supported in the composite tube wall. Neglecting the effects of tube wall inertia (a standard assumption in water hammer models [1]), the radial force balance implies that the internal pressure must be balanced by the hoop tension. Due to the winding angle of the fibers being less than 90°, the stress in the hoop direction is transmitted along the fibers, resulting in an axial contraction accompanying the radial expansion. The computations of radial and axial strain as a function of winding angle by Spencer and Hull [9] show that in the case of unconstrained axial motion (they treated the static case and did not consider wave motion), significant axial strain of the opposite sign to the hoop strain will occur for angles between 45° and 60°. This explains why the peak amplitude of the hoop and axial strains are very close in magnitude but of opposite sign in Fig. 4. Although the wall-thickness slightly varies for each woven pattern, the wall-thickness variations within patterns I to III are too small to result in noticeable differences in wave speed. However, as anticipated from previous static failure studies [9], these patterns exhibit very different failure modes and thresholds for tests [6] at higher projectile velocities.

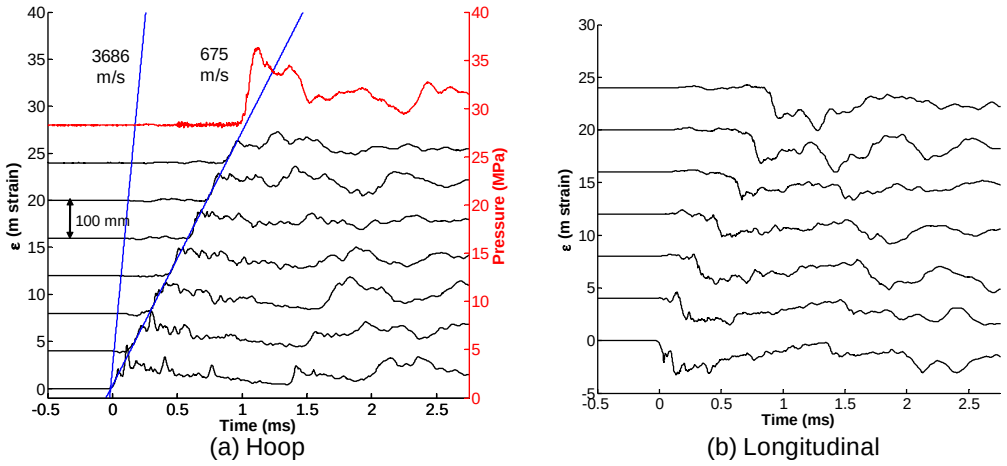

Figure 4: Strain and pressure histories for shot 075, CFC 45° tube, wall-thickness 1.66 mm, pattern I.

Comparing with the tube of 45° winding angle, the tube of 60° has a shorter pitch of fiber strands and thus becomes stronger in hoop direction. The precursor wave and the primary wave propagate at 2777 m/s and 1062 m/s, respectively. Consistent with the previous discussion, the precursor wave of the 60° tube is slower and the primary wave faster than those of the 45° tube. The peak strains for hoop and axial directions are 1.9 $m$strain and -2.7 $m$strain, so that ratio ϵ_A/ϵ_H = -1.4, larger than the 45° case.

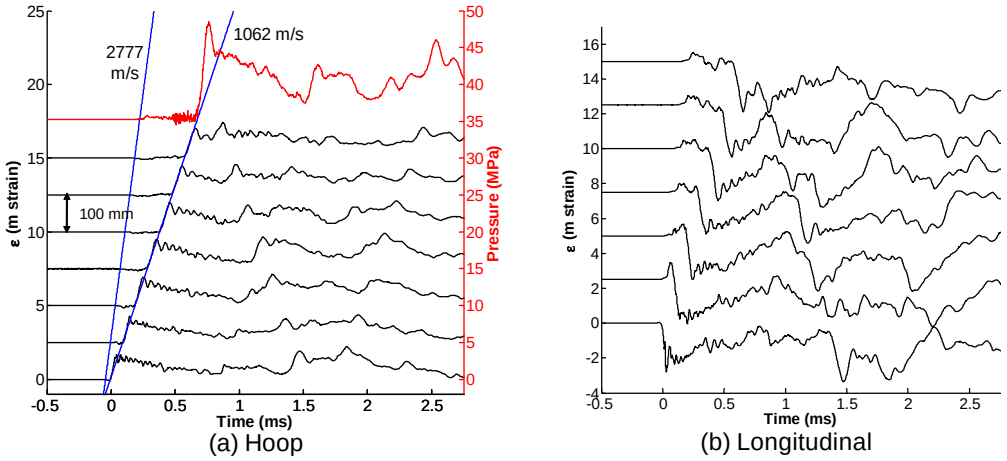

Figure 5: Strain and pressure histories for shot 070, CFC 60° tube, wall-thickness 1.65 mm, pattern I.

Shots 112 and 113 were conducted with the GRP tube which has a winding angle of 50°. Figure 6 shows hoop and axial strain histories in shot 113. Precursor and primary wave velocities measured for the axial and hoop wave fronts are 2367 m/s and 888 m/s. In shot 113, averaged frontal peaks of hoop and axial strains are 1.5 $m$strain and -0.6 $m$strain. The results for the GRP tube are inconsistent with the CRP tube for several reasons. First, the fiber and matrix properties, particularly the volume loading of fibers, are obviously different for the GRP and CRP specimens. Second, the friction between the GRP specimen tube and buffer appears to transmit a substantial axial stress wave directly to the tube from the impact event. This creates a axial strain precursor that is initially negative in amplitude (compression), contrary to the previous CFC tube results which show a tension precursor. We believe that this is due to an excessively tight gland seal on the buffer since in the other experiments with a looser grand seal, the axial precursor has a positive amplitude [3]. Only the precursor wave appears to be significantly influenced by this effect. The primary wave appears to be essentially independent of the friction and determined solely by the

tube geometry and tube material in accord with the Korteweg model, Eqs. 1 and 2. The magnitude of stress wave does depend on the buffer friction due to water squirting past a loose seal. In shots 112 and 113, the primary wave amplitude is reduced because the buffer seal was looser.

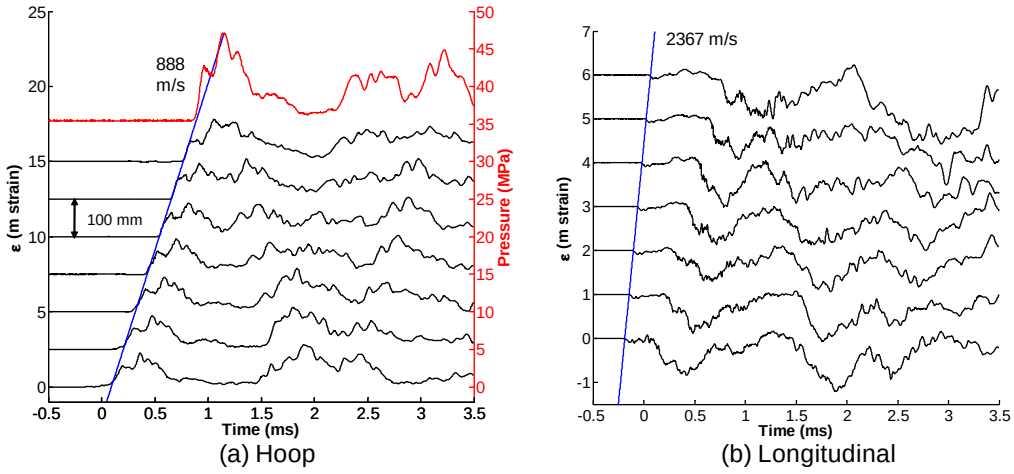

Figure 6: Strain and pressure histories for shot 113, GRP 50° tube, wall-thickness 1.60 mm, helical winding.

Predicted composite properties and comparison with classical water-hammer theory

As shown in Fig. 7a, the wave speeds depend strongly on the winding angle. We know of no published theoretical treatment[1] for the precursor and Korteweg wave speeds in general composite materials. However, we can estimate the wave speeds using the laminate theory of composite stiffness to estimate the mechanical properties of the tubes. Our estimates are based on the models developed by Puck and his co-workers for fiber-reinforced plastics; the models are described by Greenwood [10] and Hull and Clyne [11]. Using their analysis of stresses in individual plies, we have calculated the effective Young's modulus (Fig. 7b) for hoop and axial directions, E_H and E_A, using property data given in Table 2. We have estimated the precursor and primary wave speeds using the effective modulus relevant to that mode of propagation. For the precursor waves, the effective axial modulus E_A is used to estimate the precursor wave speed as $\sqrt{E_A/\rho_s}$. For the primary wave, the Korteweg speed is estimated from the standard water-hammer theory of Eqs. 2 evaluating β using the effective hoop modulus E_A in Eq. 1. Figure 7a compares these predictions for the precursor and primary with wave speeds obtained in shots 066-108.

The predicted dependence of wave speeds on the winding angle are in reasonable agreement with the experimental results. The precursor wave speed becomes slower with increasing winding angle while the primary wave speed becomes faster. This is due to the load being primarily carried in tension along the fibers. In terms of the laminate theory, the effective modulus in the hoop direction becomes much larger than in the axial direction with increasing winding angle, Fig. 7b. In a wave propagation situation such as the present experiments, tension waves propagate primarily along the fiber so that on purely geometrical grounds, we expect that with increasing winding angle, the tension in the fiber has to propagate a longer time to progress a given axial distance, which gives the effect of a slower precursor speed.

We can estimate the effective CRP tube Young's modulus for the hoop direction using the experimentally measured primary wave speed and the Korteweg expression, Eqs 1 and 2. The results are shown in Fig. 7b. As shown, there is reasonable agreement the predicted trend although the estimated modulus falls below the predicted value by 30 to 60%. A more refined model of the composite material and correct treatment of the dynamics is needed in order to make a quantitative comparison. Similar estimates can be made for the GRP tube and we have determined that the effective Young's modulus for the hoop direction is about 30 GPa. This is about 10% higher than the nominal value of 27.6 GPa given by Watters [12].

[1]Jeong Ho You and Kauschik Bhattacharya of CIT have recently developed a theoretical treatment that extends the four-equation model of water hammer by computing the elastic properties of the composite tube using a standard laminate model of the composite material.

Table 2: Material properties of CFC tube.

Fiber		
Young's modulus	E_f	238 GPa
Density	ρ_f	1770 kg/m^3
Poisson's ratio*	ν_f	0.3
Matrix		
Tensile modulus	E_m	2.83 GPa
Density	ρ_m	1208 kg/m^3
Tensile Poisson's ratio*	ν_m	0.280
Composite		
Volume fraction of fiber	V_f	0.7

*Data from Hull and Clyne[11]

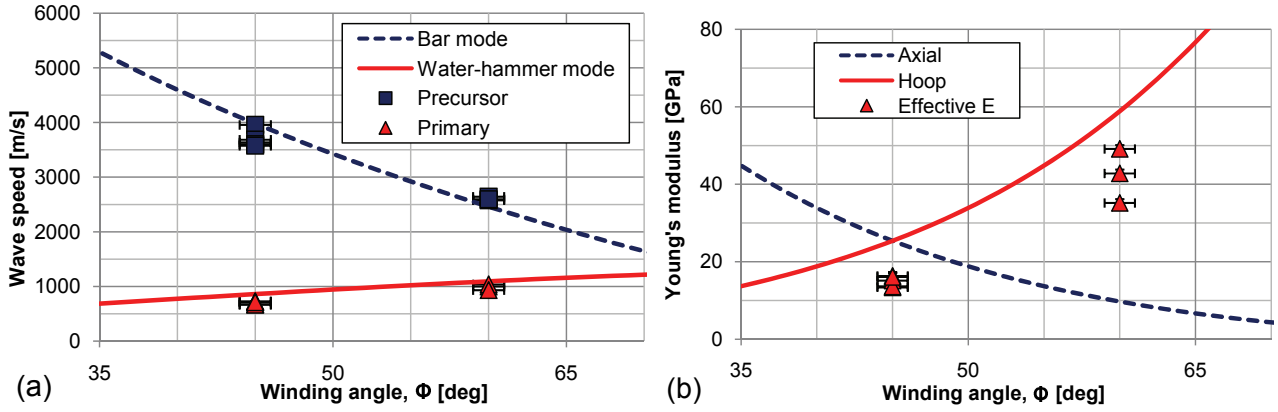

Figure 7: Predicted and experimental dependence on the winding angle (a) primary and precursor wave speeds (b) predicted/effective Young's modulus.

3 Summary

We used projectile impact to study the propagation of coupled structural and pressure waves in water-filled composite tubes. The results are qualitatively similar to our previous work on water-filled metal tubes in that we observe a coupled structural-fluid wave corresponding to the Korteweg wave of water hammer. The main disturbance travels at a Korteweg speed that is consistent with the effective modulus for the hoop direction of deformation for both CFP and GFP tubes. The precursor waves travel at a speed consistent with a bar wave motion and the effective axial modulus. The coupling of the hoop and axial deformation is much stronger for composite than metal tubes and is observed to vary systematically with winding angle. The observed coupling and the propagation speed of precursor and primary waves are consistent with the laminate theory of fiber reinforced composites.

Acknowledgements

This research was sponsored by the Office of Naval Research, DOD MURI on Mechanics and Mechanisms of Impulse Loading, Damage and Failure of Marine Structures and Materials (ONR Grant No. N00014-06-1-0730), program manager Dr. Y. D. S. Rajapakse. We thank Tomohiro Nishiyama of Japan Patent Office for his help in conducting experiments. Mike Kaneshige of Sandia National Laboratories provided substantial assistance with the gun design.

References

[1] Wiggert, D. C., and Tijsseling, A. S., 2001. "Fluid transients and fluid-structure interaction in flexible liquid-filled piping". *Applied Mechanics Reviews,* **54**(5), pp. 455–481.

[2] Inaba, K., and Shepherd, J. E., 2008. "Flexural waves in fluid-filled tubes subject to axial impact". In Proceedings of the ASME Pressure Vessels and Piping Conference. July 27-31, Chicago, IL USA. PVP2008-61672.

[3] Inaba, K., and Shepherd, J. E., 2008. "Impact generated stress waves and coupled fluid-structure responses". In Proceedings of the SEM XI International Congress & Exposition on Experimental and Applied Mechanics. June 2-5, Orlando, FL USA. Paper 136.

[4] Lighthill, J., 1978. *Waves in Fluids*. Cambridge University Press.

[5] Shepherd, J. E., 2006. "Structural response of piping to internal gas detonation". In ASME Pressure Vessels and Piping Conference., ASME. PVP2006-ICPVT11-93670, presented July 23-27 2006 Vancouver BC Canada.

[6] Inaba, K., and Shepherd, J. E., 2009. "Failure of liquid-filled filament-wound tube subjected to axial impact loading". In ICCM-17 17th International Conference on Composite Materials., ICCM. to be presented July 27-31 2009, Edinburgh, UK.

[7] Beltman, W. M., Burcsu, E., Shepherd, J., and Zuhal, L., 1999. "The structural response of cylindrical shells to internal shock loading". *Journal of Pressure Vessel Technology*, pp. 315–322.

[8] Beltman, W. M., and Shepherd, J., 2002. "Linear elastic response of tubes to internal detonation loading". *Journal of Sound and Vibration,* **252**(4), pp. 617–655.

[9] Spencer, B., and Hull, D., 1978. "Effect of winding angle on the failure of filament wound pipe". *Composites,* **9**, pp. 263–271.

[10] Greenwood, R. P., 1977. "German work on grp design". *Composites,* **7**, pp. 175–184.

[11] Hull, D., and Clyne, T. W., 1996. *An Introduction to Composite Materials*, 2nd ed. Cambridge University Press.

[12] Watters, G. Z., 1984. *Analysis and Control of Unsteady Flow in Pipelines*. Butterworth Publishers, MA.